

Multi-layer haemocompatible diamond-like carbon coatings obtained by combined radio frequency plasma enhanced chemical vapor deposition and magnetron sputtering

A. C. Popa · G. E. Stan · M. A. Husanu · I. Pasuk ·
I. D. Popescu · A. C. Popescu · I. N. Mihailescu

Received: 12 February 2013 / Accepted: 28 July 2013 / Published online: 13 August 2013
© Springer Science+Business Media New York 2013

Abstract: Radio-frequency Plasma Enhanced Chemical Vapour Deposition (in different methane dilutions) was used to synthesize adherent and haemocompatible diamond-like carbon (DLC) films on medical grade titanium substrates. The improvement of the adherence has been achieved by interposing a functional buffer layer with graded composition Ti_xTiC_{1-x} ($x = 0-1$) synthesized by magnetron co-sputtering. Bonding strength values of up to ~ 67 MPa have been measured by pull-out tests. Films with different sp^3/sp^2 ratio have been obtained by changing the methane concentration in the deposition chamber. Raman spectroscopy, X-ray photoelectron spectroscopy and X-ray diffraction were employed for the physical-chemical characterization of the samples. The highest concentration of sp^3-C ($\sim 87\%$), corresponding to a lower DLC surface energy (28.7 mJ/m²), was deposited in a pure methane atmosphere. The biological response of the DLC

films was assayed by a state-of-the-art biological analysis method (surface enhanced laser desorption/ionization–time of flight mass spectroscopy), in conjunction with other dedicated testing techniques: Western blot and partial thromboplastin time. The data support a cause-effect relationship between sp^3-C content, surface energy and coagulation time, as well as between platelet-surface adherence properties and protein adsorption profiles.

1 Introduction

The amorphous phase of sp^3 bonded C atoms is known in literature as “diamond-like carbon” (DLC) [1–3]. DLC is an extremely tough and resistant material and is used in the form of thin films, usually for coating metal parts exposed to high friction [4, 5]. Common methods of DLC films synthesis are plasma enhanced chemical vapour deposition [6–8], filtered pulsed arc discharge [9, 10], magnetron sputtering [2, 11], ion beam deposition [12] and pulsed laser deposition [13, 14].

Besides high wear resistance coatings for metallic parts, DLC also proved useful in coating implants due to some specific surface properties (low surface energy values and chemical inertness) that prevent blood coagulation and favour osteoblasts adhesion [1, 15]. The higher the sp^3 content in DLC, the larger the internal stress in thin films [16] causing peeling from substrate. Two main solutions were reported for improving the bonding strength: synthesis of (i) multilayer structures (e.g. Ti–TiN–TiC–DLC) [17, 18] or of (ii) functionally graded materials [19–21]. The head of the femoral prosthesis is made of alloys with high wear resistance (Co–Cr). Inside the human body, the friction with the acetabular cup is accentuated by the presence of liquids that attack the metal and enhance the

A. C. Popa
Army Centre for Medical Research, 020012 Bucharest, Romania

A. C. Popa
Department of Cellular and Molecular Medicine, “Carol Davila”
University of Medicine and Pharmacy, 050474 Bucharest,
Romania

A. C. Popa · G. E. Stan (✉) · M. A. Husanu · I. Pasuk
National Institute of Materials Physics,
077125 Magurele-Bucharest, Romania
e-mail: george_stan@infim.ro

I. D. Popescu
“Victor Babes” National Institute of Pathology,
050096 Bucharest, Romania

A. C. Popescu · I. N. Mihailescu
National Institute for Lasers, Plasma and Radiation Physics,
077125 Magurele-Bucharest, Romania

wear rate. DLC proved biocompatible and can be applied as a protective layer against wear and as a barrier against metal ion release [1, 22].

However, in the biomedical field, the main necessity for DLC coatings comes however from vascular prostheses. In the case of interaction with blood it seems that DLC quality has a major influence upon clotting time. During the blood flow through these tubes, the erythrocytes and thrombocytes (platelets) aggregate in certain spots and may eventually block the blood passage. To compensate for this general weakness of vascular prostheses, DLC films can bind albumin molecules from the sanguine plasma forming a passive layer that makes the surfaces less adhesive for blood platelets [23].

The blood compatibility with carbon-based films is extremely complex and for the moment there is no relation found between haemocompatibility and surface properties such as surface energy, atomic bond structure of carbon or composition of material. Contradictory data have been reported regarding the behaviour of the material in terms of blood clotting, the adherence of platelets or protein adsorption to the surfaces.

The relationship between the sp^3 bonds content of DLC and its anti-thrombogenicity properties is still not well understood. Many *in vitro* [2] and *in vivo* [13, 24] studies indicate that better results can be obtained for a higher sp^3 content. Nevertheless, an opposite trend has also been reported for: (i) tetrahedral amorphous carbon films deposited by pulsed vacuum arc [25], and (ii) hydrogenated amorphous carbon (a-C:H) films deposited by plasma immersion ion implantation, when the blood compatibility tended to improve with the increase of sp^2/sp^3 ratio [26].

Kwok et al. [27] pointed out that a higher surface energy of phosphorous doped a-C:H films is associated with a low adsorption of proteins, among them the albumin being the preferential one. Similar findings in terms of protein adsorption were presented by Ma et al. [28] who reported a higher albumin to fibrinogen adsorption ratios on surfaces with higher surface energy. On the other hand Hasebe et al. [29, 30] observed that haemocompatibility improves with the decrease of surface energy due to fluorine incorporation in DLC films. Saito et al. [31] also observed that the increase in hydrophobicity increases the anti-thrombogenicity of their fluorinated DLC films. Jones et al. [32] explored platelet attachment on Ti, TiN, TiC and DLC surfaces and reported that the more hydrophilic surfaces present a greater platelet spreading and fibrinogen adsorption. They suggested that the better haemocompatibility of DLC surface is linked to its low surface energy and thus high hydrophobicity. Okpalugo et al. [33] also noted that improved blood compatibility can be obtained when surface energy is lowered in silicon doped a-C:H films.

We report on the fabrication of highly adherent multilayer coatings $Ti/Ti_xTiC_{1-x}/DLC$ using combined radio-frequency magnetron co-sputtering and plasma enhanced chemical vapour deposition, with an intermediate buffer layer having a gradual composition (Ti_xTiC_{1-x} ; $x = 0-1$) synthesized by a new approach [34, 35]. We studied the correlation between activated partial thromboplastin time (aPTT) and surface energy of DLC structures with different sp^3/sp^2 bonds ratio. Attention was paid to the investigation of protein adsorption and platelets adherence to the surface, both acting as crucial factors for material haemocompatibility.

2 Materials and methods

2.1 Substrate preparation

Mirror-polished titanium (Mateck GmbH) discs ($\Phi = 15$ mm) were used as deposition substrates. The substrates were ultrasonically cleaned in acetone and iso-propanol for 10 min and then dried in argon flow.

2.2 Deposition procedure

The DLC structures were deposited with a UVN-75R1 (1.78 MHz) type system equipped with two RF magnetron cathodes and with one plasma enhanced chemical vapour deposition (PECVD) position. This configuration allows preparing different kinds of structures, like composites, multilayer or graded structures by using both magnetron sputtering (MS) and PECVD deposition methods (Fig. 1). Because of the well-known poor adherence of the DLC films to metallic substrates, we attempted a new architectural coating design: a functionally graded structure (FGS). MS was used to obtain the FGS adherence buffer layer, and PECVD to prepare the top biofunctional DLC film.

The FGS buffer layer was prepared by co-sputtering from two targets, titanium (Ti) and titanium carbide (TiC), in a pure argon atmosphere (0.35 Pa pressure). The Ti and TiC targets were fixed on the vertical and on the horizontal cathode, respectively (Fig. 1). Initially, the substrate holder was placed in a parallel position to the Ti target, at a separation distance of 50 mm. During the deposition process, it was gradually displaced towards the TiC target by a planetary movement. The rotating holder was placed in five different equidistant positions between the Ti and the TiC targets, each for a 3-min deposition time. This way we fabricated a structure with composition gradient (Ti_xTiC_{1-x}) finished with titanium carbide surface. After the 15 min of co-sputtering a 30 nm thick Ti_xTiC_{1-x} functional layer with graded composition was obtained (as determined by X-ray Reflectometry measurements performed on a structure deposited on a glass substrate).

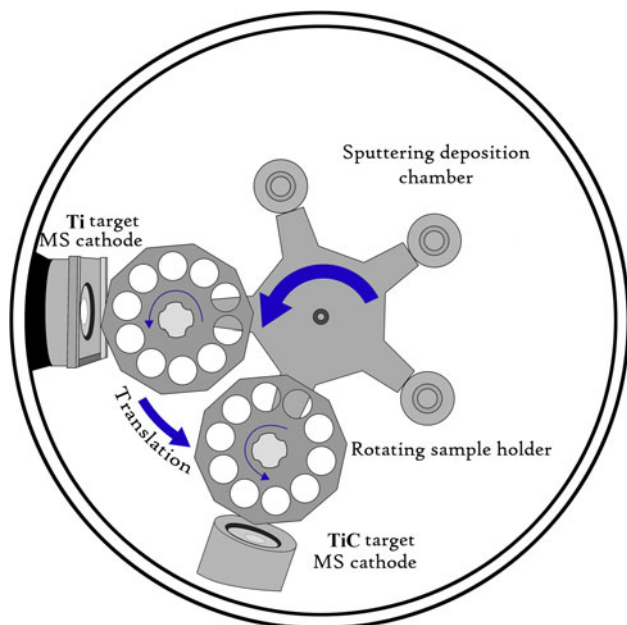


Fig. 1 Schematic diagram of magnetron co-sputtering deposition set-up

In a second session, the deposited structures were fixed with silver paint onto the PECVD horizontal cathode. The DLC structures were prepared using three different dilutions of methane in argon (20, 60 and 100 %) at a total pressure of 15 Pa. The samples are further denoted as D20, D60, and D100, respectively. During deposition, the DC_{bias} value was kept at ~ 400 V. When the RF power of 75 W was supplied, the substrate temperature increased due to plasma bombardment, but never exceeding 50°C , as monitored with a Chromel–Alumel thermocouple system.

For comparison, samples without the $\text{Ti}_x\text{TiC}_{1-x}$ graded buffer layer were deposited in identical conditions.

Prior to each deposition session the chamber was evacuated down to a base pressure of $\approx 10^{-4}$ Pa.

2.3 Characterization techniques

2.3.1 Morphology and composition

The DLC films thickness was measured by profilometry.

In order to study the vibrations of carbonic matrix, Raman spectroscopy measurements were performed with a Renishaw 1,000 micro Raman system excited with the 532 nm line of an Elforlight laser diode operating at 30 mW. For each sample, a set of 20 measurements of 5 s integration time were performed.

XPS analysis, indicating the C 1s core level variation was used in order to assess the amount of sp^2 and sp^3 bonded C in the three types of samples (D20, D60, and D100). XPS spectra were recorded in a dedicated chamber

(Specs, Germany), under ultra high vacuum (base pressure $\sim 10^{-10}$ mbar), using Al $K_{\alpha} = 1486.71$ eV monochromatized radiation. The electrons were collected using a hemispherical electron energy analyzer (Phoibos 150) operated at a 30 eV pass energy. Resolution (in terms of full width at half maximum) of 0.45 eV was achieved. During measurements, a flood gun operating at 1 eV acceleration energy and 100 μA electron current was used in order to ensure sample neutralization. The spectra were recorded both prior and after sputter cleaning for 10 min using an ion current of 10 μA in order to analyse the ion-beam induced changes in the surface composition and bonding. During sputtering, the pressure inside the XPS analysis chamber was kept at 1×10^{-7} mbar. The experimental data were fitted with Voigt profiles, allowing different values for the background. C 1s line ($E = 284.5$ eV) was used as reference for the charge shift correction.

The crystallographic structure of each film was investigated by X-ray diffraction (XRD), using a *Bruker D8 Advance* diffractometer, in parallel beam setting, equipped with copper anode X-ray tube. The measurements were carried out in grazing incidence geometry at 1° in the 2θ range from 20° to 65° , with a step size of 0.04° and 90 s acquisition time per step.

2.3.2 Pull-out bonding strength

The pull-out measurements were carried out using a DFD Instruments PAT MICRO AT101 (maximum pull force=1 kN) adhesion tester equipped with 2.8 mm diameter stainless steel test elements. The test elements were glued to the film surface with E1100S cyanoacrylate one-component epoxy adhesive. The stub surface was first polished, ultrasonically degreased in acetone and ethanol and dried in a nitrogen flow. After gluing, the samples were placed in an oven for thermal curing ($130^\circ\text{C}/1$ h). Each test element was pulled-out vertically with a calibrated hydraulic pump until detachment. The experimental procedure was conducted in accordance with the ASTM D4541-09e1 standard. The mechanical adhesion strength was determined from the recorded failure value divided by the quantified detached surface area. Five samples were tested independently for each type of deposition condition. Mean value and standard deviation were computed.

2.3.3 Surface energy

We performed solid surface energy calculations based on contact angle measurements, using deionized water and formamide as standard solvents. The measurements of the prepared DLC structures were carried out using a goniometric method, the two solvents being dropped onto the surface and the contact angle estimated. The drop size and

the drip distance were kept constant in all cases. The contact angle values were determined by the evaluation of the tangent angle of a sessile liquid drop on the DLC solid surface. The surface energy was calculated using the Owens–Wendt approximation [36, 37]. Five experiments were performed for each DLC surface. Mean value and standard deviation were computed.

2.3.4 Biological assays

2.3.4.1 Important note In order to eliminate the potential biological variations, blood was prelevated from 5 healthy non-smoking patients. They signed an informed consent allowing us to use their blood and derivatives of their blood in our studies in accordance with the ethical rulings of the Helsinki declaration (6th revision, World Medical Association 59th Meeting, Seoul 2008).

2.3.4.2 Surface preparation Surfaces were cleaned in ultrasonic bath with 80 % ethanol. Then, surfaces involved in cell testing were sterilized by autoclavation (for 30 min, at 130 °C and 0.1 MPa) in individual sealed sterilization bags. All procedures were carried out in a sterile environment and all biohazard safety measures were used.

2.3.4.3 Whole blood, plasma and platelets solutions We have sampled blood in standard test-tubes with or without anticoagulant substances (sodium citrate or ethylenediaminetetraacetic (EDTA)).

2.3.4.4 Partial thromboplastin time test In order to assess interaction with blood coagulation systems, we conducted a slightly modified protocol for manual detection of aPTT as introduced by Margolis [38]: fresh blood was harvested in sodium citrate (3.2 % final concentration) using Vacutainer medical devices from five healthy non-smoking patients.

Prior to the test, CaCl_2 was added to plasma to counter the effects of sodium citrate and enable clotting. The samples were placed on a plane surface and drops of plasma (50 μl) were deposited from a distance of 1 cm. The aPTT was considered as the time for plasma clotting on surface [38, 39].

For comparison of DLC coatings characteristics with commercial biomaterials, the same analysis was performed on medical grade poly(methyl-methacrylate) (PMMA) and Ti plates. Five experiments were performed for each type of surface. Mean value and standard deviation were computed.

2.3.4.5 Platelet adhesion quantification Healthy patients' blood was collected in Vacutainer tubes containing EDTA as anticoagulant. Platelets were obtained by centrifugation of whole blood. First, tubes were centrifuged at $250\times g$ for

5 min, at room temperature in order to separate red and white blood cells. Then, the platelet-rich plasma was removed and centrifuged in a second tube at $800\times g$ in order to obtain platelets. The plasma was removed and the platelets were washed three times with cell culture medium M199 and centrifuged at $800\times g$ as before. Platelets were resuspended with medium M199 at a density of 1×10^8 platelets/ml.

300 μl medium M199 containing platelets was deposited in a uniform layer onto samples (Ti, D20, D60, D100). They were put in sterile Petri dishes and transferred in a humidified atmosphere incubator at 37 °C with 5 % CO_2 saturation. After 2 h the discs were washed twice with phosphate buffer saline and overlaid with 100 μl lysis buffer (50 mM Tris HCl, 0.15 mM NaCl, 1 % Triton X-100, 0.5 % Na Deoxicolate, 0.1 % SDS, 2 mM EDTA, 10 $\mu\text{g}/\text{ml}$ aprotinin, 10 $\mu\text{g}/\text{ml}$ pepstatin, 1 mM PMSF). The platelets lysate was centrifuged at $14,000\times g$ for 15 min, and supernatants were removed and stored at 80 °C.

2.3.4.6 Western blot analysis Samples were denaturated by boiling for 10 min in 2 % DDT. Samples of 10 μl were subjected to SDS-PAGE with 12 % acrylamide-bisacrylamide gels. The transfer was carried out in a wet cell, on polyvinylidene fluoride (PVDF) membranes in a Mini Protean system (Bio-Rad, USA). The membranes were blocked overnight in a 5 % dry milk solution in TBST (50 mM Tris/HCl, 150 mM NaCl, 0.1 % Tween-20). Incubation with anti-beta actin antibody produced in rabbit (Santa Cruz, USA) diluted 1:200 on TBS with 2 % BSA, was performed at room temperature (RT), for 1 h. After three times washing, the membranes were incubated at RT for 1 h with corresponding horseradish peroxidase (HRP) coupled secondary antibody (goat anti rabbit and goat anti mouse from Santa Cruz) at a dilution of 1:20,000. Chemiluminescence reagents (enhanced chemiluminescence kit, Pierce, USA) were added to membranes for 2 min and results were acquired on BioMax films (Kodak, USA) developed automatically according to the manufacture's indication. Membranes were stripped in 5 % beta-mercaptoethanol for 1 h at 45 °C and probed with anti-aptrotinin mouse antibody (Thermo Scientific, USA) for loading control. Film analysis was conducted with Gel Scan 7,000 and Quantity One software (both from Bio-Rad, USA).

2.3.4.7 Adsorbed protein mass spectroscopy Blood from healthy patients was collected in Vacutainer test-tubes containing EDTA, and centrifuged at $1,000\times g$ for 10 min in order to obtain fresh plasma. Plasma from five patients was pooled and 100 μl of plasma was put in contact with each type of material: Ti, D20, D60, and D100. After 1 h the discs were washed three times with ice cold double

distilled water and overlaid with 100 μl analysis buffer (7 M urea, 2 M thiourea, 2 % CHAPS, 2 % beta mercaptoethanol, 10 $\mu\text{g/ml}$ pepstatin, 1 mM PMSF). Samples were sonicated and 16 μl of each were mixed in a test tube with 4 μl energy absorbing molecule buffer (5 mg sinapinic acid dissolved in 400 μl solvent composed of: 50 % acetonitrile, 0.5 % trifluoroacetic acid, 49.5 % H_2O HPLC grade). 10 μl of each sample were loaded onto spots of ProteinChip Gold Array and allowed to dry in the laminar flow hood used for cell cultures. After drying a quantity of 1 μl energy absorbing molecule buffer was added to each spot and allowed to dry under the same conditions.

Samples were analysed with a ProteinChip Surface Enhanced Laser Desorption/Ionization-Time of Flight mass spectroscopy (SELDI-ToF) platform (Bio-Rad, USA) and ProteinChip DATA Manager software. All materials used in this experiment were purchased from Bio-Rad, USA. Parameters were: mass range 6,000–2,00,000; focus mass: 25,000; matrix attenuation: 6,000; sampling rate 400; calibration method: PCS4000 instrument default; acquisition method: SELDI Quantization; warming: energy 4,400 (1 shot); data: energy 4,000 (10 shots).

2.3.4.8 Statistical analysis For the pull-out, surface energy and aPTT measurements the statistical significance was determined using an unpaired Student's *t* test. The differences were considered significant when $p < 0.05$.

3 Results

3.1 Film thickness

Thickness measurements by profilometry revealed a linear dependence of the DLC deposition rates by PECVD on the methane dilution in the working atmosphere: 5 nm/min for D20, 9.1 nm/min for D60, and 15 nm/min for D100. For conformity of experiments, all the top biofunctional DLC layers were prepared at a 300 nm thickness.

3.2 Raman measurements

Raman spectroscopy was used to characterize the quality of the DLC films, obtained at different methane dilution, in terms of diamond carbon-phase purity (Fig. 2). This technique proved very useful in correlating the electronic properties of carbonaceous materials with their vibrational signature, given the high sensitivity of vibrational modes (located in the 1,200–1,600 cm^{-1} spectral range) to modifications in the electronic configurations of C atoms.

The Raman spectra were deconvoluted with three components, corresponding to: nanocrystalline carbon

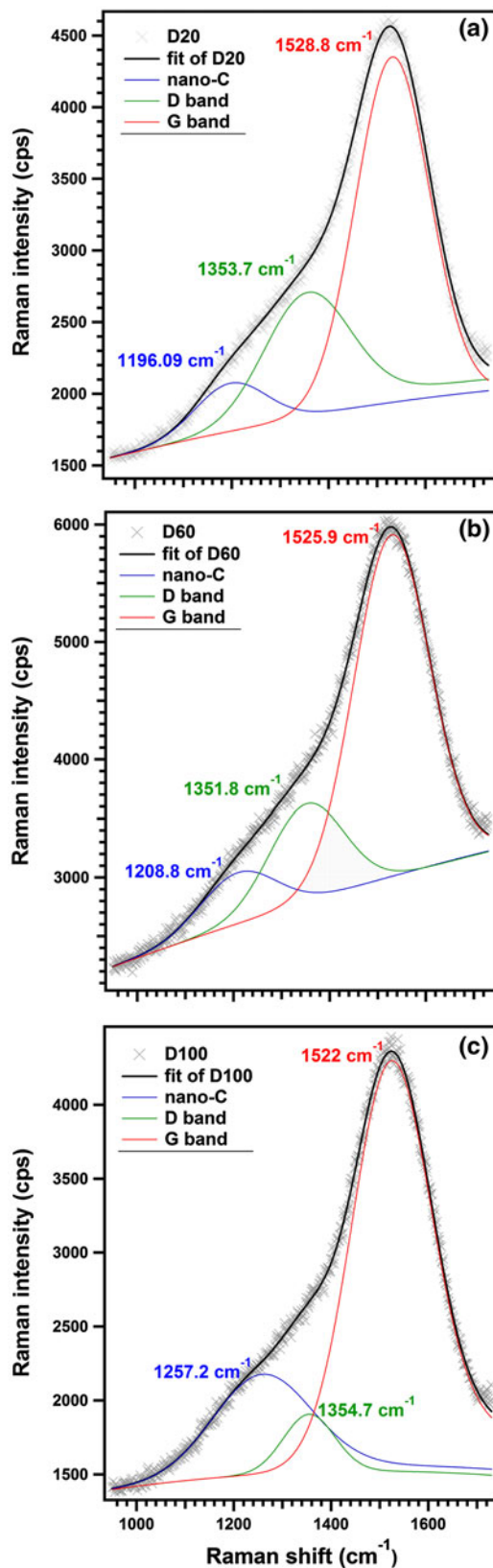


Fig. 2 Raman spectra of DLC films deposited in: **a** 20 % CH_4 + 80 % Ar atmosphere **b** 60 % CH_4 + 40 % Ar atmosphere, and **c** 100 % CH_4 atmosphere

Table 1 Raman deconvolution data for the DLC films (relative bands' intensities, FWHM, I_G/I_D ratios)

Sample	Component (%)			FWHM D band (cm^{-1})	I_G/I_D
	Nano-C	D band	G band		
D20	10.45 ± 0.24	28.46 ± 0.65	61.09 ± 1.41	206.8	~ 2.1
D60	13.19 ± 0.44	23.94 ± 0.81	62.87 ± 2.13	172.6	~ 2.6
D100	25.20 ± 1.02	15.48 ± 0.63	59.32 ± 2.12	127.8	~ 3.8

contribution, D band and G band respectively (Fig. 2). The G-peak corresponds to the fundamental E_{2g} mode of graphite, and D-peak to disordered graphite [40, 41].

The peak between 1,100 and 1,300 cm^{-1} , as in our case, is often attributed to nanocrystalline or amorphous diamond [42–45]. Accordingly, one can assume the presence of nanocrystalline diamond clusters with sp^3 -bonding embedded in the non-crystalline matrix of our carbonaceous films. In the Raman spectrum of D100 sample, an enhancement of the band associated to nanocrystalline form of C may be observed, which suggests a crystalline C form appearance.

The position of the G peak and the ratio of the integrated areas under the G and D peaks (I_G/I_D) (Table 1) is correlated with the sp^2/sp^3 bonding ratio [40, 46, 47]. The decrease of the I_G/I_D ratio, the shifting of the G peak towards higher wave numbers and the broadening of the D-peak are widely accepted as indicators for the increase of the graphite-like phase concentration in the carbon films [46, 48, 49].

We can observe that as the methane dilution is increased, the I_G/I_D ratio increases too (Fig. 2 and Table 1). According to Zhang et al. [46] and Ferrari et al. [40, 47] a higher I_G/I_D ratio corresponds to a higher percent of sp^3 -C bonds. This variation is accompanied by a slight continuous shift of the G band from $\sim 1,529 \text{ cm}^{-1}$ (D20) to $\sim 1,522 \text{ cm}^{-1}$ (D100). In the Raman spectra of carbon-based materials the G-peak positions move to higher wave numbers due to two processes: the increase of the sp^2 content and/or a higher compressive stress [50]. Additionally, the full-width at half-maximum (FWHM) of D-peak also showed a progressive decrease with the increase of methane concentration (Table 1), in good correlation with the aforementioned I_G/I_D ratio and G band position trends. Although the main indicative furnished by Raman spectroscopy concerning the sp^3 -C amount is the I_G/I_D ratio, the widening of the D-peak, which is correlated with a distribution of carbonaceous clusters having different dimensions [47], may as well serve as a structural “gauge”.

3.3 XPS characterization

From the XPS analysis we could extract the amount of sp^3 -bonded C and sp^2 -C as the ratio between the integral intensities of each component. The XPS spectra exhibited a very complex shape indicating the existence of different

chemical states for C 1s (Fig. 3). The experimental data were fitted with Voigt profiles, allowing different values for the integral background instead of using just one integrated spectrum [51]. Three components were needed in order to assure a good fit, associated with the sp^3 -C ($\sim 286 \text{ eV}$) and sp^2 -C ($\sim 284.3 \text{ eV}$) contributions, as well as to C–O, C=O and/or O=C=O bonds (287.5–289.9 eV) owing most probably to the contamination of the sample surface [52–54]. The results of the fitting are presented in Table 2.

The deconvolution studies of the C 1s spectra generally reveal two main distinct peaks assignable to sp^2 - and sp^3 -C hybridizations [54]. The peak situated at a higher binding energy (BE) is assigned to sp^3 -bonded carbon (C–C and C–H), and that at lower BE corresponds to the sp^2 hybridization state of carbon.

From the analysis of the main components of C 1s core level spectra we can conclude that the amount of sp^2 bonded C decreases from $\sim 36 \%$ in D20 sample to about 10 % in D100 sample.

We note that the result for D20 sample is in agreement with the Raman measurements which suggested that a higher content of sp^2 is present in these films. When the methane dilution is increased (D60 and D100) the sp^3 -C concentration strongly increases (to around 78 and 87 %, respectively).

3.4 XRD characterization

The XRD patterns of the DLC samples are presented in Fig. 4. The diffraction peak centred on $2\theta = 44.2^\circ$ ($d = 2.04 \text{ \AA}$) which appears in the patterns of samples D60 and D100 can be assigned to the most intense and unique peak of diamond (face-centred cubic, ICDD # 01-75-410) accessible in grazing incidence with the current experimental set-up ($2\theta < 65^\circ$). This is the only diffraction peak that does not belong to titanium in D60. In the case of D100 there are several other weak maxima, which fit satisfactorily to two quite unusual (obtained at high temperature and high pressure) carbon-based phases (ICDD # 46-943 and ICDD # 46-944), reported by Shterenberg and Bogdanova [55].

3.5 Pull-out test adherence

The adherence of the coating to the metallic substrate is a very important parameter for haemocompatible applications.

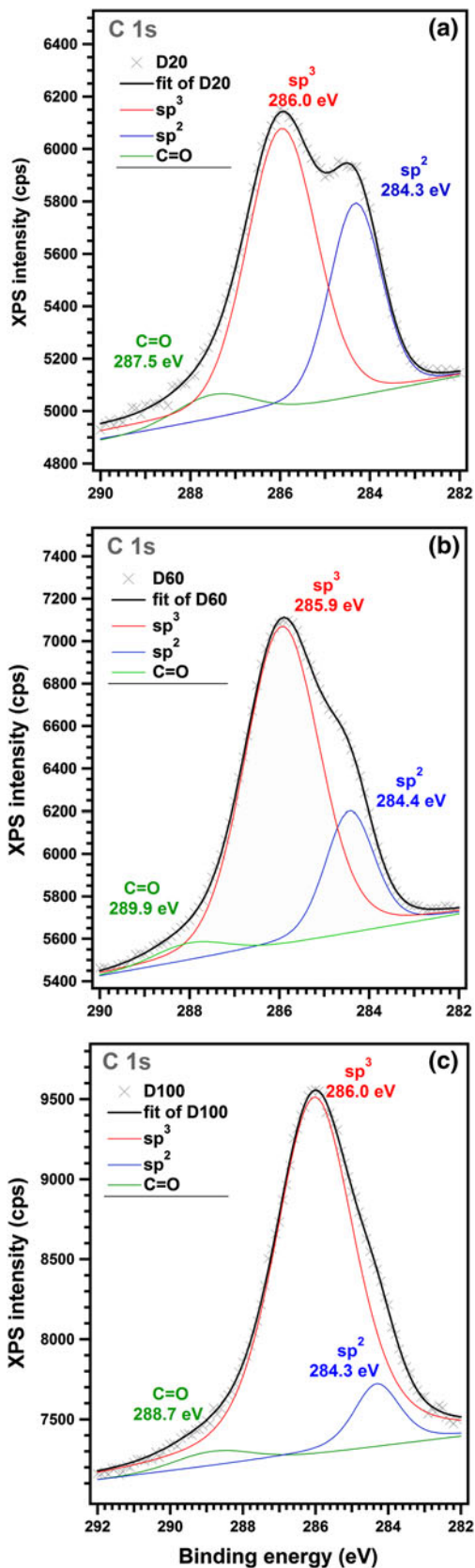


Fig. 3 High resolution XPS spectra for C 1s core level photoelectron after sputter cleaning: samples **a** D20; **b** D60; and **c** D100

Table 2 XPS peak separation data for the C 1s line of DLC films

Sample	Component (%)			sp^3/sp^2 ratio
	C=O/-COO	sp^2 -C	sp^3 -C	
D20	5.7 ± 0.3	35.9 ± 1.2	58.4 ± 2.0	~ 1.6
D60	4.3 ± 0.2	17.3 ± 0.6	78.4 ± 2.4	~ 4.5
D100	2.8 ± 0.15	9.7 ± 0.5	87.5 ± 3.4	~ 9.0

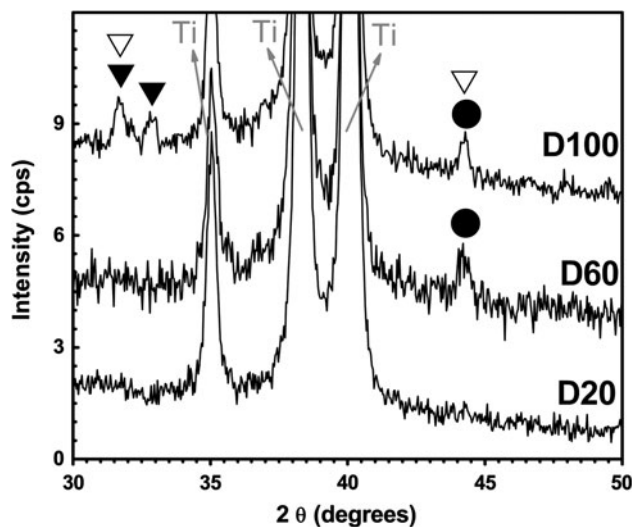


Fig. 4 GIXRD patterns of the $Ti/Ti_xTiC_{1-x}/DLC$ structures [filled circle–Diamond (ICDD # 01-75-410); filled triangle–Carbon (ICDD # 00-46-943); empty triangle–Carbon (ICDD # 00-46-944)]

A value of ~ 40 MPa is the minimum required for this kind of applications (ISO 13485:2003).

A strong enough epoxy adhesive (E1100S) was used to evaluate the suitability of the DLC coating adherence. Prior to the DLC coating adherence evaluation, the glue bonding strength was tested independently on bare titanium plates. Each time, the failure occurred in the glue volume at 80–85 MPa, confirming its technical specification.

The simple DLC/Ti structures presented unsatisfactory adherence values, well below the threshold of 40 MPa, being easily detached by a common scotch-test (D20 and D60) or even by simple scratching (D100). On the other hand, the prepared FGS coatings demonstrated promising values of adherence (Fig. 5), even higher than those required by mandatory international standards for the load-bearing orthopaedic implants (ISO 13779–2:2008). The lowest value of bonding strength (58 ± 4.2 MPa) was recorded for D100 structures. The mean adherence value increased slightly for D60 (60 ± 3.5 MPa), and more for D20 (66.7 ± 2.2 MPa) (see Fig. 5). The two tailed *t*-testing with unequal variances showed no statistically significant difference ($p > 0.05$) between the recorded adherence values of D60 and D100, whilst the difference was

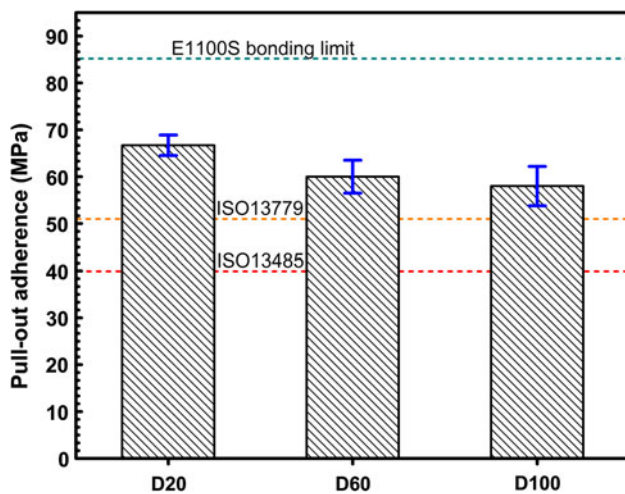


Fig. 5 Histogram depicting the variation of the mean pull-out adherence values of the DLC films

statistically significant ($p < 0.05$) between D20 versus D60 and D100.

The insertion of the co-sputtered Ti_xTiC_{1-x} transition stratum aims to reduce the interface discontinuity between the two different materials (Ti and DLC), which improves significantly the adhesion strength. The functionally graded interlayer acts as an anchor, contributing to the adaptation at the interface area. Moreover, a carbide surface can react with the depositing gaseous radicals, promoting a “chemical bonding” of the nucleating DLC layer, that can further enhance the film adhesion.

3.6 Surface energy

The surface energy values recorded for DLC/Ti structures were lower than those of the bare medical grade Ti and PMMA control substrates (Table 3). One can also notice a decrease of the surface energy with the increase of methane dilution in the reactor chamber (Table 3). The two tailed t -testing showed statistically significant differences ($p < 0.05$) between the surface energy values recorded for all the samples. An important decrease (with $\sim 25\%$) of

Table 3 Surface energy values recorded for the DLC films, and for the Ti and PMMA controls

Sample	Deposition atmosphere composition	Surface energy (mJ/m^2)
Bare Ti	N/A	37.85 ± 0.94
PMMA	N/A	36.35 ± 0.78
D20	20 % CH_4 + 80 % Ar	32.09 ± 0.73
D60	60 % CH_4 + 40 % Ar	30.50 ± 0.70
D100	100 % Ar	28.71 ± 0.34

the surface energy was obtained when applying the DLC coating: from $37.85 \pm 0.94 \text{ mJ/m}^2$ for the bare Ti substrate down to $28.7 \pm 0.34 \text{ mJ/m}^2$ for the D100 structure.

3.7 Biological assay

In order to assess the haematological biocompatibility, the coagulation time was measured, followed by more complex tests: platelet adhesion and protein adsorption to the surface.

3.7.1 aPTT tests

Generally, higher partial thromboplastin times were recorded on DLC coated surfaces with respect to two commercial control surfaces (Ti and PMMA) (see Table 4). The two tailed t -testing, assuming unequal variances, showed statistically significant differences ($p < 0.05$) between the aPTT values. A remarkably higher aPTT value was obtained in the case of D100 coating, which will be discussed later in conjunction with the other physical and biological results.

3.7.2 Platelet adhesion

The amount of beta-actin, a structural protein present in all cells, was investigated by Western blot method. The obtained signal is proportional to the quantity of beta actin and, therefore, to the number of platelets adhered on the sample surface at the moment of lysis. The PVDF membranes were also probed with aprotinin (a protease inhibitor with proteic structure and mass of $\sim 6 \text{ kDa}$) which was present in the same concentration in all samples, since it was added to the lysis buffer formulation. This is an internal quality control which ensures that all steps of the technique are properly done. As visible from Fig. 6, there was almost the same number of platelets present on the surface of bare titanium and D20 samples. The number of platelets adhered on D60 and D100 was significantly lower.

Table 4 aPTT values measured for the DLC films, and for the Ti and PMMA controls

Sample	Deposition atmosphere composition	aPTT (min)
Bare Ti	N/A	13.4 ± 0.8
PMMA	N/A	15.0 ± 0.6
D20	20 % CH_4 + 80 % Ar	16.5 ± 0.7
D60	60 % CH_4 + 40 % Ar	19.3 ± 0.8
D100	100 % Ar	24.9 ± 1.0

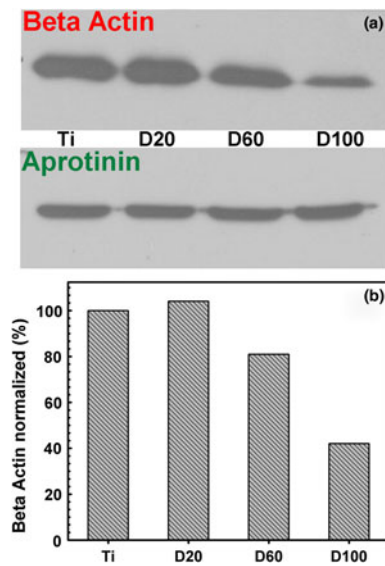


Fig. 6 **a** Western blot analysis of beta-actin and aprotinin present in platelets adhered on DLC and bare Ti samples; **b** Optical density histograms of normalized quantity of beta-actin present in platelets adhered on DLC and bare Ti samples

3.7.3 Protein adsorption

To study the adsorption pattern of proteins to the samples' surface a state-of-the-art technique was used: *Surface Enhanced Laser Desorption/Ionization-Time of Flight mass spectroscopy (SELDI-ToF)*.

As one can observe (Fig. 7a), serum albumin was adsorbed in greater quantities on all DLC surfaces than on the bare titanium surface [Albumin molecular weight (MW) \approx 66483 Da]. Other proteins (G immunoglobulins) presented a roughly similar pattern (G immunoglobulins MW \approx 134350 Da). Another important peak is that of 28,900 Da which can be assigned to the factor XIIa light chain and is more prominent on the titanium sample (Fig. 7b). The factor XII, the activator of surface contact coagulation cascade, could not be identified because it had a mass similar to that of albumin (Factor XII MW \approx 67792 Da).

4 Discussion

The sustainability of a biocompatible film, to be applied as biofunctional coating layer of implantological elements used to remedy various cardiologic, orthopaedic or dental medical conditions, is essentially conditioned by the adherence to substrate.

Unfortunately the high thermal expansion mismatch between DLC and Ti, responsible for the high tensile stress in the film, causes a relatively poor film adhesion (as shown in Sect. 3.5 and Refs [17, 56]). Moreover, a higher sp^3 content in the DLC films, which is believed to play an

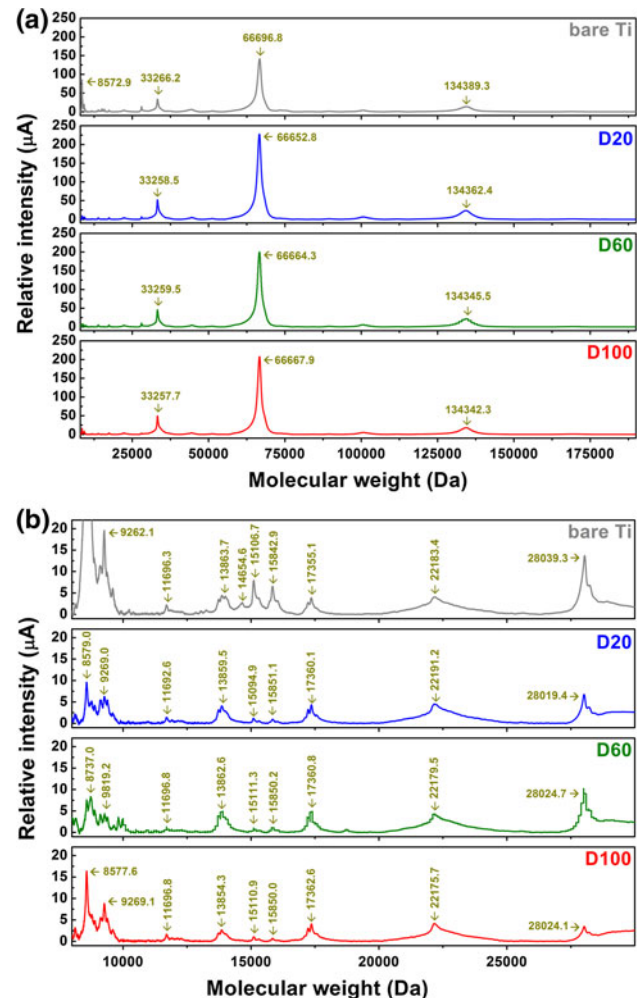


Fig. 7 **a** SELDI-ToF complete spectra of proteins adsorbed on DLC and bare Ti samples from fresh blood plasma; **b** SELDI-ToF detailed spectra in MW range 8,000–30,000 Da

important role on the blood biocompatibility, also induced greater internal stress and reduction of film adhesion [16]. The deposition of the DLC film on a rather thick inter-layer buffer (e.g., titanium carbide or titanium nitride) and not directly on the metallic surface resulted in better adherence results [17, 18, 57–59]. However, when using TiN as an intermediary buffer layer a significant haemolytic effect was observed after long assessment times [17, 18].

In this study we propose an alternative solution which resorts to the introduction of a graded transition from the titanium support to the DLC top biofunctional film by co-sputtering from two targets: Ti and TiC. The 30 nm thick Ti_xTiC_{1-x} ($x = 0-1$) buffer layer significantly improved the top DLC film adherence. The slightly lower adherence of the D100 samples, compared to D60 and D20, could be related to its higher sp^3 bond content, which can induce a higher internal stress. It is worth noting, that all the recorded pull-out adhesion values are superior to the value

imposed by the international standards for biocompatible load-bearing coatings to withstand dynamical mechanical loads (ISO 13779–2:2008; ASTM F 1185-03: 2009).

The increase in the sp^3 content with the increase of the methane concentration in the working atmosphere has been confirmed both by Raman and XPS. We measured a significant sp^3 content augmentation from sample D20 to D100, which could be the effect of the initial sp^3 -hybridization of carbon in the methane molecule. Bugaev et al. [60] also reported that high quality DLC films can be obtained from pure methane, their results pointing that most probably methyl mechanism is favourable for diamond-like bonds formation. It is known that CH_3 are the most abundant species in pure methane discharges, while carbon dimer C_2 is the most abundant in methane highly diluted in argon discharges [61, 62]. It is not surprising, neither unprecedented [62] that at low temperature the formation of diamond-like bonds from a reactive environment having as majority species C_2 dimers is more difficult.

In order to better predict the behaviour of materials *in vivo* we designed a range of *in vitro* tests to investigate the events that happen on the surface when put in contact with blood. We first analysed the aPTT, which is generally used to detect the degree of activation of the endogenic clotting system, to measure the surface dependent blood clotting. Next, we dissociated the elements involved in coagulation—plasma and platelets—and separately investigated their interaction with surfaces.

As visible from Table 3, the surface energy is decreasing with the methane concentration in the deposition atmosphere. In DLC, the graphene regions of sp^2 carbons are heavily conjugated and partially charged boundaries appear, which could promote adsorption of charged blood proteins such as coagulation factors, kininogens, and various globulins [63]. We hypothesize that the more boundaries of graphene regions or the more distorted graphene regions exist, the more partial charges will appear, the faster the charged proteins will be adsorbed and the more quickly the blood/plasma will coagulate.

One can notice that for DLC functionalized structures the tendency of the partial thromboplastin time is to increase with the decreasing of surface energy values (Tables 3 and 4). The maximum thromboplastin time was recorded for the DLC structures prepared in pure methane atmosphere (D100). The clotting process can usually be initiated by surface adsorption and contact activation of coagulation factors of the endogenic clotting system [64]. Unlike bare Ti, the contact with the DLC coated surface suppresses the activation of the endogenic clotting system.

The adherence of platelets to the materials plays a key role in platelet activation and subsequently in blood clotting activation. Platelet adherence was studied by Western

blot analysis of beta actin, a structural protein present in all cells. In our opinion this technique allows for a more correct determination of the variations of platelet adherence than optical approaches often used in literature. However, there are some groups that have attempted to better simulate the natural conditions [65, 66], in platelet adherence studies and have assembled an enclosed system which ensures a laminar flow through parallel plates of material. This system is not infallible, since this way the blood is subjected to an important shear stress, due to circulation via a pump through tubings which can activate platelets, along with other surfaces interactions thus conducting to additional errors. As seen in the platelet adhesion experiment (Fig. 6), the DLC coatings create conditions for a weaker platelet-surface interaction, which *in vivo* can conduct to a lower platelet activation and subsequently a prolonged time of coagulation (see Fig. 8). One can assert that this effect derives from the fact that all cells have a negatively charged cellular membrane which tends to interact/adhere to positively charged surfaces (hydrophilic surfaces) rather than to hydrophobic ones.

In this work, the interaction of blood with the surface was investigated by SELDI-ToF mass spectroscopy which generates a profile of protein adsorption at interface with materials, as seen in Fig. 7.

The other current approaches in literature put the resolubilised powder of bovine serum albumin or fibrinogen in Phosphate Buffer Saline, in contact with a material and determine the adsorption. This is a rather simplistic way to study protein adsorption behaviour because these determinations are focused on one protein at once, making it difficult to predict these phenomena in their complexity. Our approach is in pace with nowadays proteomics, since it uses fresh blood plasma from healthy patients which is a

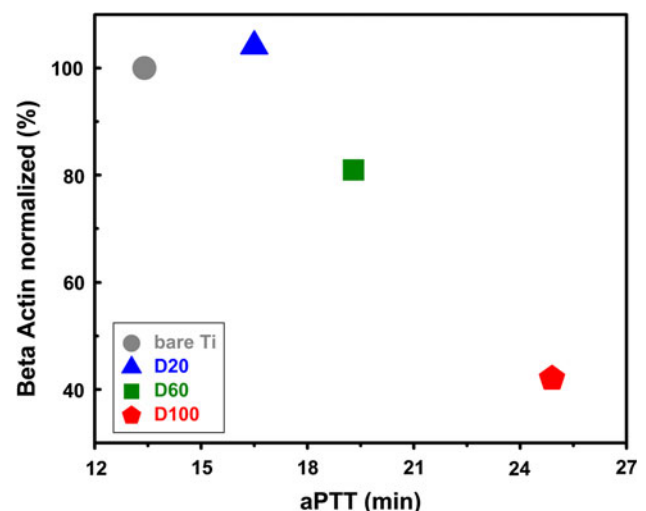


Fig. 8 The DLC coatings and Ti bare control aPTT values plotted against the normalized beta-actin values

complex mixture of proteins, peptides, aminoacids and many organic and inorganic substances.

Albumin, with a molecular weight of ~ 66.5 kDa represents roughly 50–60 % of plasma proteins and is not glycosylated like other proteins in blood. The G immunoglobulins (~ 134.5 kDa) account for roughly 15 % of plasma proteins. Fibrinogen is found at concentrations in range of 150–400 mg/dl and other coagulation factors are enzymes present in very small quantities. Albumin is a protein which has hydrophobic moieties, being a blood carrier for many hydrophobic molecules. Since our DLC surfaces tend to be more hydrophobic it is expected to find more adsorbed albumin than on titanium as confirmed by mass spectroscopy spectra. The vast majority of proteins in blood are glycosylated which makes them more hydrophilic and more susceptible to polar interactions. The quantity of albumin adsorbed on the surface shields the surface of the sample, making it difficult for the different proteins and coagulation factors to reach the sample and activate the coagulation cascade (Fig. 7b). These findings are in line with Liu et al. [67], who showed that the albumin adsorption on DLC inactivates the surface for blood clotting.

We can state that the coagulation time for each material is in line with surface energy data, with the platelet–surface adherence properties and protein adsorption profiles, and so advocates for a cause-effect relationship between these factors.

5 Conclusions

Adherent and haemocompatible DLC films have been synthesized onto titanium substrates using combined radio-frequency MS and PECVD methods. The effects of methane concentration in the reactor chamber on the structural properties of the DLC films and on the biological response of the samples can be concluded as follows:

1. The introduction of a graded transition from the titanium support to the DLC top biofunctional film by co-sputtering from two targets (Ti and TiC) through a Ti_xTiC_{1-x} ($x = 0-1$) buffer layer resulted in a significant improvement of the DLC films' adherence. The adherence values are similar to or even higher than those imposed by international standards and are therefore encouraging for implantology applications.
2. The sp^3 content increased with the methane concentration in the deposition atmosphere.
3. The relationship between the sp^3 content and anti-thrombogenicity of DLC films was confirmed by the partial thromboplastin time. The haemocompatibility is strongly dependent on the methane concentration: a higher concentration of methane reduces the platelet activation and thrombus formation;
4. We studied protein adsorption using fresh blood plasma from healthy patients. In the case of DLC films with the highest sp^3 content albumin was preferentially adsorbed (due to the affinity between surface and the hydrophobic moieties of this protein), thus shielding the surface and preventing the immobilization of coagulation factors.

Next, wear/abrasion measurements together with antimicrobial tests are projected in order to fully assess this coating design feasibility for implantology development.

Acknowledgments This work was supported by the Romanian National Authority for Scientific Research through the PNII-RU-TE-2011-3-0164 (TE 49/2011). A.C. Popescu is grateful for the financial support of PNII-RU-TE-2012-3-0379 (TE 16/2013). The authors thank Eng. D.A. Marcov for helping with the coatings' preparation.

References

1. Roy RK, Lee KR. Biomedical applications of diamond-like carbon coatings: a review. *J Biomed Mater Res B*. 2007;83:72–84. doi:10.1002/jbm.b.30768.
2. Logothetidis S. Haemocompatibility of carbon based thin films. *Diamond Relat Mater*. 2007;16:1847–57. doi:10.1016/j.diamond.2007.05.012.
3. Ostrikov K, Cvelbar U, Murphy AB. Plasma nanoscience: setting directions, tackling grand challenges. *J Phys D*. 2011;44:174001. doi:10.1088/0022-3727/44/17/174001.
4. Heimberg JA, Wahl KJ, Singer IL, Erdemir A. Superlow friction behavior of diamond-like carbon coatings: Time and speed effects. *Appl Phys Lett*. 2001;78:2449. doi:10.1063/1.1366649.
5. Donnet C, Erdemir A. *Tribology of diamond-like carbon films: Fundamentals and applications*. Berlin: Springer; 2007.
6. Petersen M, Bandorf R, Brauer G, Klages CP. Diamond-like carbon films as piezoresistors in highly sensitive force sensors. *Diamond Relat Mater*. 2012;26:50–4. doi:10.1016/j.diamond.2012.04.004.
7. Oliveira EC, Cruz SA, Aguiar PHL. Effect of PECVD deposition parameters on the DLC/PLC composition of a-C:H thin films. *J Brazil Chem Soc*. 2012;23:1657–62.
8. Vaghri E, Khalaj Z, Ghoranneviss M, Borghei M. Characterization of diamond-like carbon films synthesized by DC-plasma enhanced chemical vapor deposition. *J Fusion Energy*. 2011;30:447–52. doi:10.1007/s10894-011-9406-8.
9. Myllymaa S, Kaivosoja E, Myllymaa K, Sillat T, Korhonen H, Lappalainen R, Konttinen YT. Adhesion, spreading and osteogenic differentiation of mesenchymal stem cells cultured on micropatterned amorphous diamond, titanium, tantalum and chromium coatings on silicon. *J Mater Sci–Mater Med*. 2010;21:329–41. doi:10.1007/s10856-009-3836-8.
10. Soininen A, Levon J, Katsikogianni M, Myllymaa K, Lappalainen R, Konttinen YT, Kinnari TJ, Tiainen VM, Missirlis Y. In vitro adhesion of staphylococci to diamond-like carbon polymer hybrids under dynamic flow conditions. *J Mater Sci–Mater Med*. 2011;22:629–36. doi:10.1007/s10856-011-4231-9.
11. Flege S, Hatada R, Ensinger W, Baba K. Properties of hydrogenated DLC films as prepared by a combined method of plasma

- source ion implantation and unbalanced magnetron sputtering. *J Mater Res.* 2012;27:845–9. doi:[10.1557/jmr.2011.341](https://doi.org/10.1557/jmr.2011.341).
12. Srinivasan S, Tang Y, Li YS, Yang Q, Hirose A. Ion beam deposition of DLC and nitrogen doped DLC thin films for enhanced haemocompatibility on PTFE. *Appl Surf Sci.* 2012;258:8094–9. doi:[10.1016/j.apsusc.2012.04.178](https://doi.org/10.1016/j.apsusc.2012.04.178).
 13. Jelínek M, Smetana K, Kocourek T, Dvůránková B, Zemek J, Remsa J, Luxbacher T. Biocompatibility and sp^3/sp^2 ratio of laser created DLC films. *Mater Sci Eng, B.* 2010;169:89–93. doi:[10.1016/j.mseb.2010.01.010](https://doi.org/10.1016/j.mseb.2010.01.010).
 14. Písářík P, Jelínek M, Smetana K Jr, Dvůránková B, Kocourek T, Zemek J, Chvostová D. Study of optical properties and biocompatibility of DLC films characterized by sp^3 bonds. *Appl Phys A.* 2013;112:143–8. doi:[10.1007/s00339-012-7216-8](https://doi.org/10.1007/s00339-012-7216-8).
 15. Nelea V, Jelínek M, Mihailescu. Chapter 18: Biomaterials: new issues and breakthroughs for biomedical applications. In: Eason R, editor. *Pulsed laser deposition of thin films: applications-lead growth of functional materials.* New York: Wiley; 2007. p. 421–59.
 16. Morshed MM, Cameron DC, McNamara BP, Hashmi MSJ. Pretreatment of substrates for improved adhesion of diamond-like carbon films on surgically implantable metals deposited by saddle field neutral beam source. *Surf Coat Technol.* 2003;174–175:579–83. doi:[10.1016/S0257-8972\(03\)00701-1](https://doi.org/10.1016/S0257-8972(03)00701-1).
 17. Liu X, Chu PK, Ding C. Surface modification of titanium, titanium alloys, and related materials for biomedical applications. *Mater Sci Eng, R.* 2004;47:49–121. doi:[10.1016/j.mser.2004.11.001](https://doi.org/10.1016/j.mser.2004.11.001).
 18. Jones MI, McColl IR, Grant DM, Parker KG, Parker TL. Haemocompatibility of DLC and TiC–TiN interlayers on titanium. *Diamond Relat Mater.* 1999;8:457–62. doi:[10.1016/S0925-9635\(98\)00426-9](https://doi.org/10.1016/S0925-9635(98)00426-9).
 19. Wei Q, Sankar J, Narayan J. Structure and properties of novel functional diamond-like carbon coatings produced by laser ablation. *Surf Coat Technol.* 2001;146–147:250–7. doi:[10.1016/S0257-8972\(01\)01394-9](https://doi.org/10.1016/S0257-8972(01)01394-9).
 20. Voevodin AA, Zabinski JS. Superhard, functionally gradient, nanolayered and nanocomposite diamond-like carbon coatings for wear protection. *Diamond Relat Mater.* 1998;7:463–7. doi:[10.1016/S0925-9635\(97\)00214-8](https://doi.org/10.1016/S0925-9635(97)00214-8).
 21. Zheng YF, Liu D, Liu XL, Li L. Ti–TiC–TiC/DLC gradient nanocomposite film on a biomedical NiTi alloy. *Biomed Mater.* 2008;3:044103. doi:[10.1088/1748-6041/3/4/044103](https://doi.org/10.1088/1748-6041/3/4/044103).
 22. Ong SE, Zhang S. Chapter 2: Amorphous carbon coatings in biological applications. In: Zhang S, editor. *Biological and biomedical coatings Handbook. Volume 2: Applications.* Boca Raton: CRC Press; 2012. p. 45–111.
 23. Fedel M, Motta A, Maniglio D, Migliaresi C. Surface properties and blood compatibility of commercially available diamond-like carbon coatings for cardiovascular devices. *J Biomed Mater Res B.* 2009;90:338–49. doi:[10.1002/jbm.b.31291](https://doi.org/10.1002/jbm.b.31291).
 24. Kocourek T, Jelínek M, Vorlíček V, Zemek J, Janča T, Žížková V, Podlaha J, Popov C. DLC coating of textile blood vessels using PLD. *Appl Phys A.* 2008;93:627–32. doi:[10.1007/s00339-008-4728-3](https://doi.org/10.1007/s00339-008-4728-3).
 25. Leng YX, Chen JY, Yang P, Sun H, Wan GJ, Huang N. Mechanical properties and platelet adhesion behavior of diamond-like carbon films synthesized by pulsed vacuum arc plasma deposition. *Surf Sci.* 2003;531:177–84. doi:[10.1016/S0039-6028\(03\)00487-4](https://doi.org/10.1016/S0039-6028(03)00487-4).
 26. Chen JY, Wang LP, Fu KY, Huang N, Leng Y, Leng YX, Yang P, Wang J, Wan GJ, Sun H, Tian XB, Chu PK. Blood compatibility and sp^3/sp^2 contents of diamond-like carbon (DLC) synthesized by plasma immersion ion implantation-deposition. *Surf Coat Technol.* 2002;156:289–94. doi:[10.1016/S0257-8972\(02\)00089-0](https://doi.org/10.1016/S0257-8972(02)00089-0).
 27. Kwok SCH, Wang J, Chu PK. Surface energy, wettability, and blood compatibility phosphorus doped diamond-like carbon films. *Diamond Relat Mater.* 2005;14:78–85. doi:[10.1016/j.diamond.2004.07.019](https://doi.org/10.1016/j.diamond.2004.07.019).
 28. Ma WJ, Ruys AJ, Mason RS, Martin PH, Bendavid A, Liu ZW, Ionescu M, Zreiqat H. DLC coatings: effects of physical and chemical properties on biological response. *Biomaterials.* 2007;28:1620–8. doi:[10.1016/j.biomaterials.2006.12.010](https://doi.org/10.1016/j.biomaterials.2006.12.010).
 29. Hasebe T, Shimada A, Suzuki T, Matsuoka Y, Saito T, Yohena S, Kamijo A, Shiraga N, Higuchi M, Kimura K, Yoshimura H, Kuribayashi S. Fluorinated diamond-like carbon as antithrombogenic coating for blood-contacting devices. *J Biomed Mater Res A.* 2006;76A:86–94. doi:[10.1002/jbm.a.30512](https://doi.org/10.1002/jbm.a.30512).
 30. Hasebe T, Yohena S, Kamijo A, Okazaki Y, Hotta A, Takahashi K, Suzuki T. Fluorine doping into diamond-like carbon coatings inhibits protein adsorption and platelet activation. *J Biomed Mater Res A.* 2007;83A:1192–9. doi:[10.1002/jbm.a.31340](https://doi.org/10.1002/jbm.a.31340).
 31. Saito T, Hasebe T, Yohena S, Matsuoka Y, Kamijo A, Takahashi K, Suzuki T. Anti-thrombogenicity of fluorinated diamond-like carbon films. *Diamond Relat Mater.* 2005;14:1116–9. doi:[10.1016/j.diamond.2004.09.017](https://doi.org/10.1016/j.diamond.2004.09.017).
 32. Jones MI, McColl IR, Grant DM, Parker KG, Parker TL. Protein adsorption and platelet attachment and activation on TiN, TiC and DLC coatings on titanium for cardiovascular applications. *J Biomed Mater Res.* 2000;53:2:413–21. doi:[10.1002/1097-4636\(200011\)52:2<413::AID-JBM23>3.0.CO;2-U](https://doi.org/10.1002/1097-4636(200011)52:2<413::AID-JBM23>3.0.CO;2-U).
 33. Okpalugo TIT, Ogwu AA, Maguire PD, McLaughlin JAD. Platelet adhesion on silicon modified hydrogenated amorphous carbon films. *Biomaterials.* 2004;25:239–45. doi:[10.1016/S0142-9612\(03\)00494-0](https://doi.org/10.1016/S0142-9612(03)00494-0).
 34. Sima LE, Stan GE, Morosanu CO, Melinescu A, Ianculescu A, Melinte R, Neamtu J, Petrescu SM. Differentiation of mesenchymal stem cells onto highly adherent radio frequency-sputtered carbonated hydroxylapatite thin films. *J Biomed Mater Res A.* 2010;95A:1203–14. doi:[10.1002/jbm.a.32947](https://doi.org/10.1002/jbm.a.32947).
 35. Stan GE, Popescu AC, Mihailescu IN, Marcov DA, Mustata RC, Sima LE, Petrescu SM, Ianculescu A, Trusca R, Morosanu CO. On the bioactivity of adherent bioglass thin films synthesized by magnetron sputtering techniques. *Thin Solid Films.* 2010;518:5955–64. doi:[10.1016/j.tsf.2010.05.104](https://doi.org/10.1016/j.tsf.2010.05.104).
 36. Owens DK, Wendt RC. Estimation of the surface free energy of polymers. *J Appl Polym Sci.* 1969;13:1741–7. doi:[10.1002/app.1969.070130815](https://doi.org/10.1002/app.1969.070130815).
 37. Roy RK, Choi HW, Yi JW, Moon MW, Lee KR, Han DK, Shin JH, Kamijo A, Hasebe T. Hemocompatibility of surface-modified, silicon-incorporated, diamond-like carbon films. *Acta Biomater.* 2009;5:249–56. doi:[10.1016/j.actbio.2008.07.031](https://doi.org/10.1016/j.actbio.2008.07.031).
 38. Margolis J. The kaolin clotting time: a rapid one-stage method for diagnosis of coagulation defects. *J Clin Pathol.* 1958;11:406–9.
 39. McGlasson DL, Brey RL, Strickland DM, Patterson WR. Differences in kaolin-clotting times and platelet counts resulting from variations in specimen processing. *Clin Lab Sci.* 1989;2:109–10.
 40. Ferrari AC. Determination of bonding in diamond-like carbon by Raman spectroscopy. *Diamond Relat Mater.* 2002;11:1053–61. doi:[10.1016/S0925-9635\(01\)00730-0](https://doi.org/10.1016/S0925-9635(01)00730-0).
 41. Ferrari AC. Raman spectroscopy of graphene and graphite: disorder, electron–phonon coupling, doping and nonadiabatic effects. *Solid State Commun.* 2007;143:47–57. doi:[10.1016/j.ssc.2007.03.052](https://doi.org/10.1016/j.ssc.2007.03.052).
 42. Morshed MM, Cameron DC, McNamara BP, Hashmi MSJ. Pretreatment of substrates for improved adhesion of diamond-like carbon films on surgically implantable metals deposited by saddle field neutral beam source. *Surf Coat Technol.* 2003;174–175:579–83. doi:[10.1016/S0257-8972\(03\)00701-1](https://doi.org/10.1016/S0257-8972(03)00701-1).
 43. De Barros MI, Vandenbulcke L. Plasma-assisted chemical vapor deposition process for depositing smooth diamond coatings on titanium alloys at moderate temperature. *Diamond Relat Mater.* 2000;9:1862–6. doi:[10.1016/S0925-9635\(00\)00335-6](https://doi.org/10.1016/S0925-9635(00)00335-6).
 44. Morshed MM, McNamara BP, Cameron DC, Hashmi MSJ. Stress and adhesion in DLC coatings on 316L stainless steel deposited

- by a neutral beam source. *J Mater Process Technol.* 2003; 143–144:922–6. doi:[10.1016/S0924-0136\(03\)00246-2](https://doi.org/10.1016/S0924-0136(03)00246-2).
45. Schwan J, Ulrich S, Batori V, Ehrhardt H, Silva SRP. Raman spectroscopy on amorphous carbon films. *J Appl Phys.* 1996;80: 440–7. doi:[10.1063/1.362745](https://doi.org/10.1063/1.362745).
 46. Zhang S, Zeng XT, Xie H, Hing P. A phenomenological approach for the I_d/I_g ratio and sp^3 fraction of magnetron sputtered a-C films. *Surf Coat Technol.* 2000;123:256–60. doi:[10.1016/S0257-8972\(99\)00523-X](https://doi.org/10.1016/S0257-8972(99)00523-X).
 47. Ferrari AC, Robertson J. Interpretation of Raman spectra of disordered and amorphous carbon. *Phys Rev B.* 2000;61: 14095–107. doi:[10.1103/PhysRevB.61.14095](https://doi.org/10.1103/PhysRevB.61.14095).
 48. Beghi MG, Ferrari AC, Botani CE, Libassi A, Tanner BK, Teo KBK, Robertson J. Elastic constants and structural properties of nanometre-thick diamond-like carbon films. *Diamond Relat Mater.* 2002;11:1062–7. doi:[10.1016/S0925-9635\(01\)00642-2](https://doi.org/10.1016/S0925-9635(01)00642-2).
 49. Ahmad I, Roy SS, Rahman MA, Okpalugo TIT, Maguire PD, McLaughlin JA. Substrate effects on the microstructure of hydrogenated amorphous carbon films. *Curr Appl Phys.* 2009;9:937–42. doi:[10.1016/j.cap.2008.09.006](https://doi.org/10.1016/j.cap.2008.09.006).
 50. Shin JK, Lee CS, Lee KR, Eun KY. Effect of residual stress on the Raman-spectrum analysis of tetrahedral amorphous carbon films. *Appl Phys Lett.* 2001;78:631. doi:[10.1063/1.1343840](https://doi.org/10.1063/1.1343840).
 51. Mardare D, Luca D, Teodorescu CM, Macovei D. On the hydrophilicity of nitrogen-doped TiO₂ thin films. *Surf Sci.* 2007;601:4515–20. doi:[10.1016/j.susc.2007.04.156](https://doi.org/10.1016/j.susc.2007.04.156).
 52. Yan XB, Xu T, Yang SR, Liu HW, Xue QJ. Characterization of hydrogenated diamond-like carbon films electrochemically deposited on a silicon substrate. *J Phys D.* 2004;37:2416–24. doi:[10.1088/0022-3727/37/17/012](https://doi.org/10.1088/0022-3727/37/17/012).
 53. Okpalugo TIT, Papakonstantinou P, Murphy H, McLaughlin J, Brown NMD. High resolution XPS characterization of chemical functionalized MWCNTs and SWCNTs. *Carbon.* 2005;43: 153–61. doi:[10.1016/j.carbon.2004.08.033](https://doi.org/10.1016/j.carbon.2004.08.033).
 54. Liao JX, Liu WM, Xu T, Xue QJ. Characteristics of carbon films prepared by plasma-based ion implantation. *Carbon.* 2004;42: 387–93. doi:[10.1016/j.carbon.2003.11.013](https://doi.org/10.1016/j.carbon.2003.11.013).
 55. Shterenberg LE, Bogdanova SV. Effect of nickel on the graphitization of carbon materials at high pressures and temperatures. *Inorg Mater.* 1979;15:632–6.
 56. Rats D, Vandenbulcke L, Herbin R, Benoit R, Erre R, Serin V, Sevely J. Characterization of diamond films deposited on titanium and its alloys. *Thin Solid Films.* 1995;270:177–83. doi:[10.1016/0040-6090\(95\)06913-5](https://doi.org/10.1016/0040-6090(95)06913-5).
 57. Park SS, Lee JY. Synthesis of diamond films on titanium substrates by hot-filament chemical vapor deposition. *J Appl Phys.* 1991;69:2618. doi:[10.1063/1.348653](https://doi.org/10.1063/1.348653).
 58. Ianno NJ, Dillon RO, Ali A, Ahmad A. Deposition of diamond-like carbon on a titanium biomedical alloy. *Thin Solid Films.* 1995;270:275–8. doi:[10.1016/0040-6090\(95\)06710-8](https://doi.org/10.1016/0040-6090(95)06710-8).
 59. Baek SH, Mihec DF, Metson JB. The deposition of diamond films by combustion assisted CVD on Ti and Ti-6Al-4V. *Chem Vap Deposition.* 2002;8:29–34. doi:[10.1002/1521-3862\(20020116\)8:1<29:AID-CVDE29>3.0.CO;2-Q](https://doi.org/10.1002/1521-3862(20020116)8:1<29:AID-CVDE29>3.0.CO;2-Q).
 60. Bugaev SP, Korotaev AD, Oskomov KV, Sochugov NS. Properties of diamond-like films obtained in a barrier discharge at atmospheric pressure. *Tech Phys.* 1997;42:945–9. doi:[10.1134/1.1258759](https://doi.org/10.1134/1.1258759).
 61. Riccardi C, Barni R, Fontanesi M, Tosi P. Gaseous precursors of diamond-like carbon films in CH₄/Ar plasmas. *Chem Phys Lett.* 2000;329:66–70. doi:[10.1016/S0009-2614\(00\)00949-0](https://doi.org/10.1016/S0009-2614(00)00949-0).
 62. Valentini L, Kenny JM, Mariotto G, Tosi P. Deposition of hydrogenated amorphous carbon films from CH₄/Ar plasmas: Ar dilution effects. *J Mater Sci.* 2001;36:5295–300. doi:[10.1023/A:1012422618327](https://doi.org/10.1023/A:1012422618327).
 63. Urbani A, Sirolli V, Lupisella S, Levi-Mortera S, Pavone B, Pieroni L, Amoroso L, Di Vito R, Bucci S, Bernardini S, Sacchetta P, Bonomini M. Proteomic investigations on the effect of different membrane materials on blood protein adsorption during haemodialysis. *Blood Transfus.* 2012;10:s101–12. doi:[10.2450/2012.014S](https://doi.org/10.2450/2012.014S).
 64. Yang P, Kwok SCH, Chu PK, Leng YX, Chen JY, Wang J, Huang N. Haemocompatibility of hydrogenated amorphous carbon (a-C:H) films synthesized by plasma immersion ion implantation-deposition. *Nucl Instrum Methods Phys Res Sect B.* 2003;206:721–5. doi:[10.1016/S0168-583X\(03\)00871-1](https://doi.org/10.1016/S0168-583X(03)00871-1).
 65. Krishnan LK, Varghese N, Muraleedharan CV, Bhuvaneshwar GS, Derangère F, Sampeur Y, Suryanarayanan R. Quantitation of platelet adhesion to Ti and DLC-coated Ti in vitro using 125-I-labeled platelets. *Biomol Eng.* 2002;19:251–3. doi:[10.1016/S1389-0344\(02\)00029-1](https://doi.org/10.1016/S1389-0344(02)00029-1).
 66. Hauert R. A review of modified DLC coatings for biological applications. *Diamond Relat Mater.* 2003;12:583–9. doi:[10.1016/S0925-9635\(03\)00081-5](https://doi.org/10.1016/S0925-9635(03)00081-5).
 67. Liu Y, Li Z, He Z, Chen D, Pan S. Structure and blood compatibility of tetrahedral amorphous hydrogenated carbon formed by a magnetic-field-filter plasma stream. *Surf Coat Technol.* 2007;201:6851–6. doi:[10.1016/j.surfcoat.2006.09.021](https://doi.org/10.1016/j.surfcoat.2006.09.021).